CHEMISTRY OF MATERIALS
Article
pubs.acs.org/cm

Synthesis of N-Heterocyclic Stannylene (Sn(II)) and Germylene (Ge(II)) and a Sn(II) Amidinate and Their Application as Precursors for Atomic Layer Deposition

Sang Bok Kim,[†,⊥] Prasert Sinsermsuksakul,[†,⊥] Adam S. Hock,[§,¶,⊥] Robert D. Pike,[‡] and Roy G. Gordon*[,†]

[†]Department of Chemistry & Chemical Biology, Harvard University, Cambridge, Massachusetts 02138, United States
[‡]Department of Chemistry, The College of William & Mary, Williamsburg, Virginia 23187, United States
[§]Department of Biological and Chemical Sciences, Illinois Institute of Technology, Chicago, Illinois 60616, United States
[¶]Chemical Sciences and Engineering Division, Argonne National Laboratory, Argonne, Illinois 60439, United States

Supporting Information

ABSTRACT: Thin films containing germanium or tin have a great variety of current and potential applications, particularly their oxides or chalcogenides. Chemical vapor deposition (CVD) and atomic layer deposition (ALD) are popular ways to make these thin films conformally even on challenging nanostructured substrates. The success of these processes depends on having precursors that are sufficiently stable, volatile, and reactive. In this paper we optimize the syntheses of the following three precursors: **1** and **2** are racemic Ge(II) or Sn(II) cyclic amides made from N^2,N^3-di-*tert*-butylbutane-2,3-diamine, and **3** is bis(*N*,*N*′-diisopropylacetamidinato)tin(II). All three compounds are demonstrated to be effective precursors for ALD of their monosulfides, GeS or SnS, by reaction with H_2S. **2** has also been reported previously to make polycrystalline SnO_2 by ALD with oxidizing agents such as H_2O_2. The cyclic amides **1** and **2** are more volatile than the amidinate **3**, vaporizing sufficiently for ALD even at precursor temperatures below 40 °C, whereas **3** vaporizes at temperatures over 90 °C. **1** and **2** can thus be used at lower substrate temperatures than **3**. GeS or SnS can be deposited on substrates even at temperatures below 50 °C, while ALD of SnS from **3** becomes slow below substrate temperatures of 100 °C because of insufficient vapor pressure. The amount of growth per ALD cycle is higher for the cyclic amide **2** than for the amidinate **3**. The GeS films are smooth and amorphous, while the SnS films are polycrystalline and granular. All of these films are uniformly thick inside holes with aspect ratios (depth/diameter) greater than 40:1.

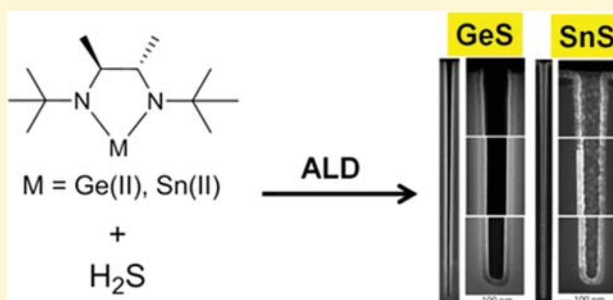

1. INTRODUCTION

Metal chalcogenides have attracted increasing interest for their electrical and optical properties.[1] Tin chalcogenides (sulfide, selenide, telluride) and tin oxide are being used in many applications. Tin oxide[2−5] has attracted great attention due to its high transparency, infrared reflectivity, and semiconductor property with an ~3.62 eV band gap. The unique properties of tin oxide have been applied to energy-conserving windows for buildings,[6] gas sensors,[7] and transparent conductive electrodes in thin film solar cells.[8−10] Germanium chalcogenides such as GeS and GeSe have attracted attention for their applications (e.g., optical waveguides and photovoltaic devices).[1,11] One of their possible applications is in phase change nonvolatile memories (PCRAM). $Ge_2Sb_2Te_5$ (GST) is the most well-known and popular phase change material for PCRAM.[12−16] Many of the potential PCRAM structures call for deposition of GST film conformally in deep trenches and pores.[17−19]

Recently, other metal chalcogenides have attracted attention for solar cell applications. The currently developed solar cells made from CdTe,[20] PbTe,[21] and Cu(In,Ga)$(S,Se)_2$[22] have problems (e.g., toxicity and limited availability) despite their promising results. In particular, the toxicity of cadmium and lead and their potential exposure are considered as a threat to health for CdTe and PbTe.[11] $Cu_2ZnSn(Se,S)_4$[22,23] is one of the most promising Earth abundant photovoltaic absorbers with 11.1% solar conversion efficiency,[23] satisfying both toxicity and scalability problems by using abundant Cu, Zn, and Sn elements. Metal monochalcogenides such as SnS,[11,24−30] SnSe,[11,31−33] GeS,[11] and GeSe[11] are being studied for their possible application to solar cells due to their low toxicity, economical large scale production, and a simpler chemistry compared to $Cu_2ZnSn(Se,S)_4$.

During device fabrication or preparation of functional surfaces, formation of conformal and uniform films on substrates in a highly controlled manner is important in obtaining reproducible desired properties. Sputtering and

Received: November 25, 2013
Revised: February 24, 2014
Published: March 12, 2014

ACS Publications © 2014 American Chemical Society

chemical vapor phase deposition methods are currently used in the formation of metal, metal oxide, metal nitride, and metal chalcogenide thin films, in the fabrication of many kinds of devices. Under the umbrella of chemical vapor phase deposition methods are chemical vapor deposition (CVD) and atomic layer deposition (ALD). ALD, previously known as atomic layer epitaxy (ALE), is a modified form of CVD for deposition of thin films.[34,35] ALD differs from CVD insofar as the vapor phase precursors arrive onto the substrate alternately via a pulse sequence; the precursor pulses are separated by periods of purging with inert gas. The film growth is performed by the surface reaction between species formed on the surface and incoming precursors by alternating depositions of pairs of precursors. In each step, once the surface reaction is complete, any excess precursor can no longer participate in the surface reaction and is removed with inert gas during purging periods. As a result, the film growth is self-limiting due to surface saturation, making homogeneous reactant flux unnecessary.

The self-limiting character of ALD[35] allows for easy and accurate control of film thickness at the atomic layer level and provides not only excellent large area uniformity but also high conformality on complex shape surfaces such as lithographically patterned surfaces and narrow holes. In order to deposit films by ALD, precursors should be compounds that can perform the surface saturation reactions. The first requirement for an optimal precursor compound for ALD is that it should be highly reactive not only toward the surfaces of substrates but also toward the surface products of the complementary precursors such as H_2S, H_2O_2, O_3, NH_3, or chalcogen metal complexes[14] (e.g., alkylsilyl compounds of tellurium and selenium). Second, precursors should be volatile at certain (relatively low) temperatures and thermally stable at the film growth temperature. In order for precursors to react at the surface of a substrate, they should not decompose until they arrive at the surface of the substrate in the ALD chamber heated at the film growth temperature. Third, any surface reaction byproducts should be nonreactive toward the surface and noncorrosive so as not to etch the thin film.

Based on these requirements for ALD precursors, *rac-N,N*′-di-*tert*-butyl-2,3-dimethylenediamine[36−38] was chosen as a suitable ligand for precursors. The bulky *tert*-butyl group on each nitrogen limits oligomerization by its steric effect. The coordination product for metal(II) using this ligand has a lower molecular weight and higher volatility[39] compared to metal(II) amidinate complexes having two amidinate ligands. Finally, the bidentate chelating effect is expected to increase the thermal stability of the cyclic metal amide complexes (*N*-heterocyclic stannylene and germylene) compared to that of monodentate metal amide complexes.

To date, three metal−organic complexes containing *rac-N,N*′-di-*tert*-butyl-2,3-dimethylenediamine have been reported: **1**,[37] **2**,[5,38,40,41] and *rac*-1,3-di-*tert*-butyl-4,5-dimethyl-1,3-diaza-2-silacyclopentane-2-ylidene.[36] The synthesis of **2** was reported almost simultaneously by Gordon et al.[5,40,41] and Russel et al.,[38] using slightly different synthetic procedures. Gordon et al. used **2** for ALD of SnO_2, and Russel et al. studied the coordination of **2** to transition metals. Russel et al. used *n*-butyl lithium to make the lithium salt of *rac-N,N*′-di-*tert*-butyl-2,3-dimethylenediamine which is afforded by the protonation of the lithiated intermediate obtained from the reaction of 1,4-di-*tert*-butyl-1,4-diaza-1,3-butadiene and methyl lithium. In contrast, bypassing isolation of the intermediate product, Gordon et al. used methyl lithium and 1,4-di-*tert*-butyl-1,4-diaza-1,3-butadiene to make the same lithium salt and allowed it to react with $SnCl_2$. For the other two compounds, intermediate coordination products are afforded by the reaction of metal chloride (H_2SiCl_2[36] or $GeCl_4$[37]) in the presence of 1,4-diazabicyclo-[2.2.2]octane (DABCO) and *rac-N,N*′-di-*tert*-butyl-2,3-dimethylenediamine, obtained from the same synthetic procedure reported by Russel et al. The final desired products were obtained from the reaction with a reducing agent, such as KC_8[36] or Li.[37] The synthetic procedure of **1** used in our group was simplified compared to that of West et al.[37] by using $GeCl_2$·dioxane and the dilithium salt of *rac-N,N*′-di-*tert*-butyl-2,3-dimethylenediamine which is prepared *in situ* from 1,4-di-*tert*-butyl-1,4-diaza-1,3-butadiene and MeLi. All the synthetic methods described above for **1** and **2** are summarized in Table S1. For ALD, the reactions of **2** with H_2O_2 and **3** with H_2S were used to deposit SnO_2[2−5] and SnS[24,29,42] films, respectively, in our group. However, detailed synthetic procedures and characterizations for both complexes (**2** and **3**) have not yet been reported.

Here, we report the synthetic procedure and characterization of **3** and simplified synthetic procedures (*in situ* synthesis) and relevant properties of compounds **1** and **2**, which may be advantageous in industrial production. We also demonstrate their reaction with H_2S to form ALD films of GeS and SnS at relatively low temperature (*ca.* 50−100 °C). It was found that the growth rate of SnS film using **2** was higher than that using **3** by *ca.* 0.3 Å/cycle. In addition, the ALD temperature window[35,43,44] of the SnS film using **2** (50−125 °C) is lower than that of **3** (100−250 °C)[42] and $Sn(acac)_2$ (125−225 °C),[30,45] enabling deposition on thermally sensitive substrates such as transparent flexible polymers.

2. EXPERIMENTAL SECTION

The procedures were performed on a Schlenk line under an atmosphere of dry nitrogen or argon inside a hood, or in a glovebox. Tin dichloride (98%, anhydrous), germanium(II) chloride dioxane complex (1:1), glyoxal solution (40 wt % in H_2O), methyllithium solution (1.6 M in diethyl ether), THF (anhydrous), pentane (anhydrous), and diethyl ether (anhydrous) were purchased from Sigma-Aldrich. *tert*-Butylamine was purchased from Acros. All chemicals were used as received. All glassware used in the experiments was dried in an oven at 160 °C. Although an ALD process for SnS using **3** was previously reported,[42] single crystal X-ray structure and other characterization such as NMR, elemental analysis, and TGA (Thermal Gravimetric Analysis) of **3** are first reported in this article.

2.1. Synthesis. *Synthesis of 1,4-Di-tert-butyl-1,4-diaza-1,3-butadiene (1,4-Diazadiene).*[46,47] A glyoxal solution (75 mL (40 w% in H_2O), 651 mmol) in distilled water (180 mL) was added dropwise via syringe to a solution of *tert*-butylamine (180 mL, 1698 mmol) in distilled water (150 mL) placed inside a round-bottom Schlenk flask (1000 mL) at room temperature. During the reaction, a solidified white product was observed in the reaction mixture. After 3 h of the reaction under nitrogen, an additional 50 mL of distilled water were added to the flask. The reaction mixture was stirred for 10 min and filtered through a fritted glass filter. The filter cake was washed three times with distilled water and air-dried with an aspirator. The crude product was dissolved in diethyl ether, and then the diethyl ether layer was decanted and evaporated. The lachrymatory white solid was dissolved in a minimum amount of diethyl ether and recrystallized on dry ice twice. The recrystallized solid product was dissolved in diethyl ether, and the solution was dried over magnesium sulfate. Afterward, magnesium sulfate was filtered out and the filtrate was evaporated resulting in a white solid. The solid product was additionally purified by sublimation at 40 °C under vacuum to give a white crystalline solid (75 g, 68%). ^1H NMR ($CDCl_3$, 500 MHz): δ 7.95 (s, 18H), δ 1.27 (s, 2H).

Scheme 1. Syntheses of ALD Precursors[a]

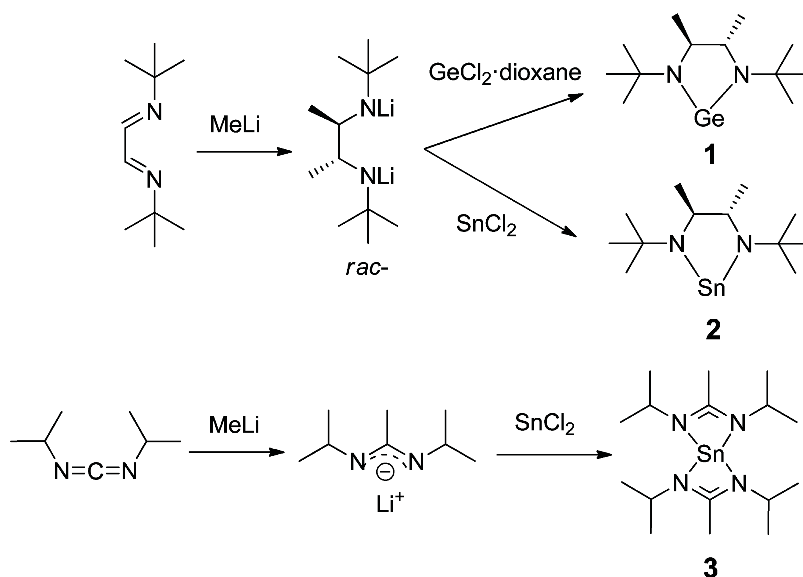

[a] *rac*-1,3-Di-*tert*-butyl-4,5-dimethyl-1,3-diaza-2-germacyclopentane-2-ylidene (**1**), also named 1,3,2-diazagermolidin-2-ylidene, 1,3-bis(1,1-dimethylethyl)-4,5-dimethyl- under CAS Registry Number 1167987-04-3; *rac*-1,3-di-*tert*-butyl-4,5-dimethyl-1,3-diaza-2-stannacyclopentane-2-ylidene (**2**), also named 1,3,2-diazastannolidin-2-ylidene, 1,3-bis(1,1-dimethylethyl)-4,5-dimethyl-, (4*R*,5*R*)-rel- under CAS Registry Number: 1268357-44-3; and bis(*N,N*′-diisopropylacetamidinato)tin(II) (**3**), also named tin, bis[*N,N*′-bis(1-methylethyl)ethanimidamidato-*κN,κN*′]-, (*T*-4)- under CAS Registry number 1421599-46-3.

Synthesis of 1, [Ge(II)(η^2-((NBu^t)CH(CH$_3$)CH(CH$_3$)(NBu^t))], rac-1,3-Di-tert-butyl-4,5-dimethyl-1,3-diaza-2-germacyclopentane-2-ylidene. MeLi (111 mL of 1.6 M, 177 mmol) was added to anhydrous diethyl ether (150 mL) in a round-bottom Schlenk flask (500 mL) under Ar atmosphere. The solution was cooled to 0 °C in an ice bath. To the solution, solid 1,4-di-*tert*-butyl-1,4-diaza-1,3-butadiene (14.53 g, 86.3 mmol) was added portionwise while stirring under a strong Ar flow over a period of 20 min. The ice bath was removed, and the reaction mixture was stirred at room temperature for 1 h. Anhydrous tetrahydrofuran was added to the diethyl ether solution of the lithiated ligand to make 300 mL of the solution. Then, the solution was transferred via cannula to an addition funnel which was connected to a round-bottom Schlenk flask (1000 mL) containing $GeCl_2$·dioxane (20 g, 86.3 mmol) and THF (200 mL) (Scheme 1). Then, the round-bottom Schlenk flask was immersed in a dry ice−acetone bath under a strong Ar flow. Using the addition funnel, addition of the lithiated ligand solution to the $GeCl_2$·dioxane in THF was performed over a period of 4 h after the flask was cooled down. After the addition was completed, the reaction mixture was kept at −78 °C for 2 h and slowly warmed up to room temperature. The reaction mixture was kept for overnight (*ca.* 12 h). The volatiles were removed on an ice bath under reduced pressure, and the crude product was extracted with pentane. The residue was washed two times with fresh anhydrous pentane. The pentane extract was evaporated on an ice−water bath under reduced pressure. The obtained crude product was distilled at 40 °C under vacuum in order to remove a colorless liquid byproduct. The desired product was distilled (60 °C, 1 Torr) to yield a pale yellow liquid (13.70 g, 59%). ^{1}H NMR (C_6D_6, 500 MHz): δ 3.02 (q, *J* = 6.0, 2H), δ 1.28 (s, 18H) 4H), δ 1.11 (d, *J* = 6.0, 6H); ^{13}C NMR (C_6D_6, 100 MHz, δ) 62.98, 55.03, 33.89, 27.46.[37]

Synthesis of 2, [Sn(II)(η^2-((NBu^t)CH(CH$_3$)CH(CH$_3$)(NBu^t))], rac-1,3-Di-tert-butyl-4,5-dimethyl-1,3-diaza-2-stannacyclopentane-2-ylidene. MeLi (100 mL of 1.6 M, 160 mmol) was added to anhydrous diethyl ether (150 mL) in a round-bottom Schlenk flask (500 mL) under Ar atmosphere. The solution was cooled to 0 °C in an ice bath. To the solution, solid 1,4-di-*tert*-butyl-1,4-diaza-1,3-butadiene (12.7 g, 75.5 mmol) was added portion-wise while stirring under strong Ar flow over a period of 20 min. The ice bath was then removed and the reaction mixture was stirred at room temperature for 1 h. Diethyl ether solution of the lithiated ligand was transferred via cannula to an addition funnel which was connected to the round-bottom Schlenk flask (1000 mL) containing anhydrous $SnCl_2$ (14.3 g, 75.5 mmol) and diethyl ether (250 mL) (Scheme 1). Then, the round-bottom Schlenk flask was immersed in a dry ice-acetone bath under strong Ar flow. After the flask was cooled down, the rate of Ar flow was reduced. Using the addition funnel, addition of the lithiated ligand solution to the $SnCl_2$ in diethyl ether was performed over a period of 4 h. After the addition was completed, the reaction mixture was kept at −78 °C for 4 h and then left on the dry ice−acetone bath without adding dry ice until the bath reached room temperature. The reaction mixture was additionally stirred overnight at room temperature. The diethyl ether was removed on an ice bath under reduced pressure, and the crude product was extracted with pentane. The residue was washed two times with fresh anhydrous pentane. The pentane extract was evaporated under reduced pressure resulting in an orange colored solid. The crude product was dried overnight at room temperature under vacuum. The solid in the Schlenk flask was transferred to a sublimator inside a glovebox. Sublimation of the crude product was performed from an oil bath kept between 45 and 50 °C, and water was used as the coolant for the coldfinger. A light-orange crystalline solid (17.8 g, 74%) was obtained. ^{1}H NMR (C_6D_6, 500 MHz): δ 3.32 (q, *J* = 6.0, 2H), δ 1.25 (s. 18H) 4H), δ 1.20 (d, *J* = 6.0, 6H); ^{13}C NMR (C_6D_6, 100 MHz, δ) 64.38, 55.99, 34.13, 28.64. EA Calcd (%): C, 45.46; H, 8.27; N, 8.84. Found (%): C, 45.35; H, 8.17; N, 8.66.

Synthesis of 3, [Sn(II)(η^2-MeC(NPr^i)$_2$)$_2$], Bis(N,N′-diisopropylacetamidinato)tin(II). 1,3-Diisopropylcarbodiimide (38.46 g or 47.72 mL, 305 mmol) was added dropwise via syringe to a methyllithium solution (200 mL of 1.6 M, 320 mmol) in anhydrous diethyl ether (250 mL) in a Schlenk flask (500 mL) on an ice bath under an argon atmosphere. The ice bath was removed 10 min after the addition, and the solution was stirred for 3 h. The lithium amidinate solution was transferred via cannula to an addition funnel connected to a round-bottom Schlenk flask (1000 mL) containing anhydrous $SnCl_2$ (28.90 g, 152 mmol) and diethyl ether (400 mL) placed on a dry ice−acetone bath (−78 °C). Using the addition funnel, the lithium amidinate was added dropwise to $SnCl_2$ in diethyl ether over a period of 2 h under a strong Ar flow. The dry ice−acetone bath was removed 30 min after complete addition, and the reaction mixture

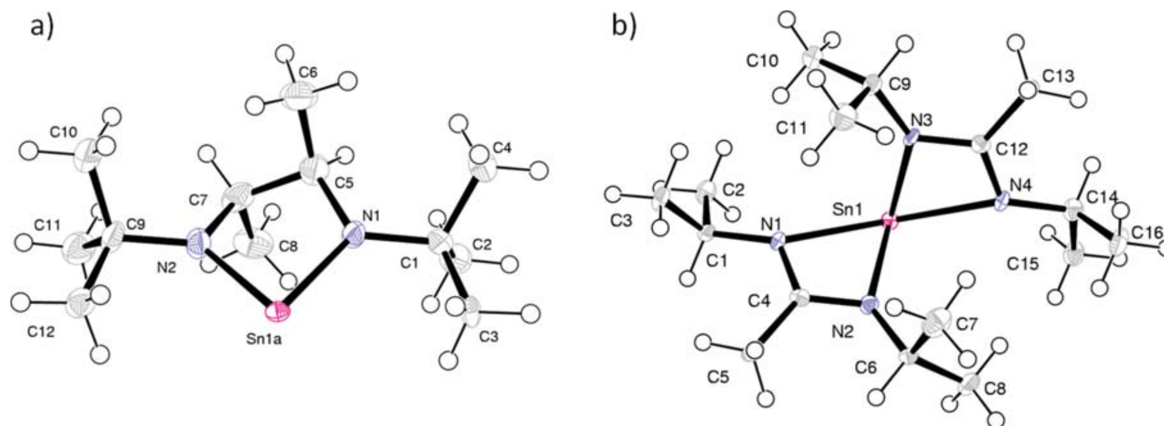

Figure 1. ORTEP plots (50% thermal ellipsoids) of the X-ray crystal structures of compounds **2** and **3**. (a) Selected bond lengths (Å) and angles (deg) for **2**. Sn(1A)−N(1) = 2.026(7), Sn(1A)−N(2) = 2.055(8), N(1)−C(5) = 1.484(12), N(2)−C(7) = 1.492(12), C(5)−C(7) = 1.520(14), N(1)−Sn(1A)−N(2) = 81.8(3), C(5)−N(1)−Sn(1A) = 113.6(6), C(1)−N(1)−Sn(1A) = 127.6(6), C(9)−N(2)−Sn(1A) = 129.1(6), C(7)−N(2)−Sn(1A) = 111.7(6), N(1)−C(5)−C(7) = 108.7(8), N(1)−C(5)−C(6) = 113.6(9), N(2)−C(7)−C(5) = 108.2(8), N(2)−C(7)−C(8) = 112.0(8). (b) Selected bond lengths (Å) and angles (deg) for **3**. Sn(1)−N(3) = 2.192(3), Sn(1)−N(2) = 2.195(2), Sn(1)−N(1) = 2.386(3), Sn(1)−N(4) = 2.388(3), N(1)−C(4) = 1.325(4), N(2)−C(4) = 1.331(4), N(3)−C(12) = 1.333(4), N(4)−C(12) = 1.324(4), N(3)−Sn(1)−N(2) = 98.12(9), N(3)−Sn(1)−N(1) = 92.88(9), N(2)−Sn(1)−N(1) = 57.82(9), N(1)−Sn(1)−N(4) = 136.40(8), C(4)−N(1)−Sn(1) = 89.80(18), C(4)−N(2)−Sn(1) = 98.24(18), N(1)−C(4)−N(2) = 113.5(3).

was stirred overnight (*ca.* 16 h). Volatiles were removed under reduced pressure, and the yellow solid residue was dissolved in pentane (*ca.* 450 mL). Insoluble organic and inorganic salts were filtered on Celite and washed with pentane under Ar. The filtrate was evaporated under reduced pressure. The resulting light yellow solid product was transferred to the sublimator inside a glovebox. The sublimation was performed at 90−95 °C under vacuum without coolant on the coldfinger (air cooling), yielding a white crystalline solid (42 g, 69%). A dark red residue was observed in the bottom of the sublimator after the sublimation was completed. In cases where a red colored or "wet" solid product was collected on the coldfinger, a second sublimation could be performed for further purification. ^{1}H NMR (C_6D_6, 500 MHz): δ 3.67 (sep, J = 6.5, 4H), δ 1.55 (s. 6H), δ 1.28 (d, J = 6.5, 24H); ^{13}C NMR (C_6D_6, 100 MHz, δ) 165.4, 47.6, 25.5, 12.2. EA Calcd (%): C, 47.90; H, 8.54; N, 13.97. Found (%): C, 47.72; H, 8.57; N, 13.99.

2.2. ALD of SnS and GeS Films. GeS and SnS thin films were deposited by atomic layer deposition (ALD) in a custom-built hot-wall ALD reactor[42,48] from the reaction of **1** or **2** with H_2S, respectively. The growth temperature was between 50 and 200 °C. The temperatures of **1** and **2** precursor sources were kept at 40 and 45 °C, which give vapor pressures of 0.71 and 0.52 Torr, respectively. A gas mixture of 4% H_2S in N_2 (Airgas Inc.) was used as the source of sulfur. H_2S is a toxic, corrosive, and flammable gas (lower flammable limit of 4%) and should be handled with caution.[49] Precursor vapors assisted by N_2 and a gas mixture of 4% H_2S in N_2 were injected sequentially into the deposition chamber to allow chemical reactions to occur successively on the substrate surface for 4 s. The purge time after precursor vapor or H_2S exposure was set to 10 s to completely remove unreacted and byproduct species and prevent reaction in the vapor phase. The deposition processes were done using the stop-flow ALD mode, reported in detailed elsewhere.[5,50]

2.3. Characterizations. *X-ray Structure Determination.* The structures of compounds **2** and **3** were determined. Diffraction quality crystals were obtained by sublimation. Crystal mounting and data collections were performed on a Siemens (Bruker) SMART CCD diffractometer using Mo Kα radiation. Data reductions were performed with SAINT, which corrects for Lorentz polarization and decay. Space groups were assigned by analysis of symmetry. Systematic absences were determined by XPREP and were further checked by PLATON. Structures were solved by direct methods and refined against all data in the 2θ ranges by full-matrix least-squares on F^2 using SHELXS-97 and SHELXL-97. Hydrogen atoms at idealized positions were included in the final refinements. Refinement details and explanations are included in the individual CIF files. Crystallographic data and final agreement factors are given in Table S2.

Thermal Gravimetric Analysis (TGA). TGA experiment was performed by the TA Instruments Model Q50 system in the glovebox. N_2 was used as a flow gas. The heating rate and mass of samples used in this experiment were set at 10 °C/min and *ca.* 40 mg, respectively.

Thin-Film Characterization. Surface morphology of the films were examined by using field-emission scanning electron microscopy (FESEM, Zeiss, Ultra-55). The film thickness was determined using a combination of cross-sectional SEM and X-ray fluorescence spectroscopy (XRF, Spectro, Xepos-III); the average thickness of rough films was determined by XRF utilizing a calibration curve of Sn $L_{\alpha 1}$ line intensity (count min^{-1}) versus the film thickness of smooth films measured by cross-sectional SEM. The elemental compositions of the films were determined by Rutherford backscattering spectrometry (RBS, Charles Evans RBS and Ionex 1.7 MV Tandetron). The crystal structures of SnS and GeS films were examined by X-ray diffraction (XRD, PANalytical X'Pert Pro) with Cu Kα radiation (λ = 1.542 Å) using θ−2θ scan.

3. RESULTS AND DISCUSSION

Because **1** is liquid, single crystal X-ray analyses were performed only for **2** and **3** (Figure 1). Crystallographic data for **2** (Table S2) exactly matched with those reported by Russel et al.[38] **2** is not a square planar type structure. The Sn atom lies out of the plane made by N1, N2, N3, and N4 (Figure S5).

Figure 2 shows that all three compounds (**1**, **2**, **3**) show very clean single-step vaporization and leave almost no residue. These TGA results mean that all three compounds vaporize or sublime without thermal decomposition. As shown in Figure 2, it was observed that cyclic type complexes (**1**, **2**) start to vaporize at lower temperature compared to **3**, the tin amidinate.

The dependence of the deposition rate of GeS and SnS on the substrate temperature was studied in the range of 50 to 200 °C to estimate the ALD window; the results are shown in Figure 3. The growth rate of SnS using **2** and H_2S (Figure 3a) was found to remain nearly constant at *ca.* 1.2 Å/cycle in the temperature range 50−125 °C and decreased by more than half to *ca.* 0.5 Å/cycle at 150−200 °C. The drop in growth rate above a certain temperature was also observed in a ALD of

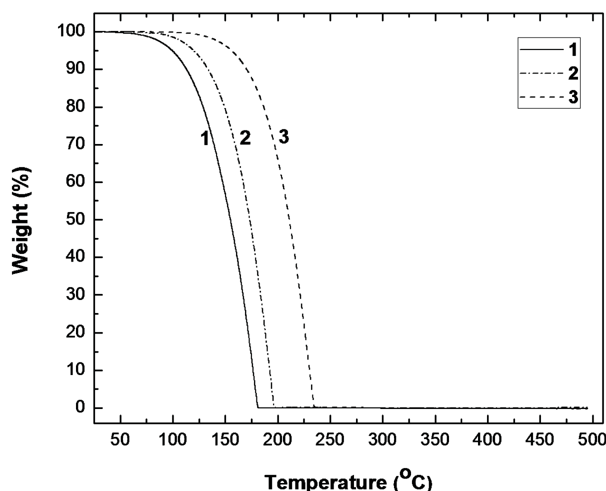

Figure 2. TGA curves of **1** (solid line), **2** (dash dotted line), and **3** (dashed line).

SnO_2 we reported previously using **2**.[3,5] There are two ways for ALD of SnO_2 using **2** as a Sn source: with hydrogen peroxide (H_2O_2) or with nitric oxide (NO). In the case of growing SnO_2 film using **2** and H_2O_2, the growth rate started to drop above 150 °C (1.8 Å/cycle) and reached *ca.* 1.2 Å/cycle at 250 °C.[5] This growth rate drop was explained by thermal decomposition of H_2O_2.[5] In the growth of SnO_2 film using **2** and nitric oxide, the growth rate started to drop above 125 °C (2.3 Å/cycle) and reached *ca.* 1.4 Å/cycle at 200 °C.[3] This growth rate, *ca.*1.4 Å/cycle, was constant from 200 to 250 °C. The growth rate drop was reported to be due to the formation of a denser SnO_2 film.[3] Because growth rate is calculated from dividing the film thickness by the number of cycles, a denser film has a lower growth rate because it is less thick compared to a lower density film. In the ALDs using both combinations of **2** and H_2O_2 and **2** and NO, an increase in growth rate due to the precursor decomposition, as in the case of **3** above 250 °C (*vide infra*),[42] was not observed up to 250 °C. This result can be translated to the thermal stability of **2**, at least, up to 250 °C. Meanwhile, the dependence of growth rate on substrate temperature for SnS using **3** and H_2S studied in our group showed that the growth rate (0.9 Å/cycle) was constant in the temperature range 100−250 °C (ALD window) and then started to increase above 250 °C.[42] This means that neither **3** nor H_2S decomposes in the temperature range below 250 °C. The increase in growth rate along with carbon contamination detected in SnS films above a substrate temperature of 250 °C was attributed to the decomposition of **3**.[42] Thus, we could conclude that **3** has thermal stability up to 250 °C as in the case of **2**.

Figure 4 shows the growth of SnS using **2** and H_2S at different temperatures. As shown in Figure 3a, the thicknesses of SnS films are significantly decreased at 150 and 200 °C (Figure 4c, d) compared to 70 °C. Furthermore, the SnS films grown at 150 and 200 °C (Figure 4c, d) have less densely packed crystalline grains, compared to those deposited at 70 °C.

From the examples of the growth rate drop described above, two conclusions can be made about the drop in the growth rate of SnS using **2** and H_2S above 125 °C. First, the drop in the growth rate is not produced by decomposition of coprecursor H_2S as in the case of ALD of SnO_2 using H_2O_2. We already know that H_2S is thermally stable at least in the range 100−250 °C from ALD of SnS using **3** and H_2S. Second, the drop in the growth rate is not caused by the formation of denser SnS film as in the case of ALD of SnS using nitric oxide (NO). As shown in Figure 4, SnS films become less dense and rougher as the temperature increases. Therefore, it is more likely that the drop in the growth rate is produced by desorption of the surface reaction product of **2** at higher temperature, although the nature of the desorbed species could not be determined in our experiments. Additionally, because the surface reaction product of H_2S in the ALD using **2** is the same as that of H_2S in the ALD using **3** (ALD window 100−250 °C),[42] it is believed that there is no desorption of surface reaction product of H_2S in the ALD of SnS using **2** in the temperature range 125−200 °C.

Unlike SnS, a constant growth rate of GeS over a wide temperature range was not observed (Figure 3b). The growth rate remained roughly constant at 0.28 Å/cycle between 50 and 75 °C. Above ∼75 °C, the growth rate of GeS decreased significantly from 0.21 Å/cycle at 100 °C to almost no growth (0.02 Å/cycle) in the temperature range 150−200 °C, indicating an increase in precursor desorption with increasing temperature as in the case of ALD SnS using **2** and H_2S. From the experiments of film growth rate vs substrate temperature for GeS and SnS (Figure 3), the optimal temperature was chosen as 70 °C in the ALD window for both compounds.

For both metal sulfide films studied, reactions between the precursor and hydrogen sulfide are self-limiting. Saturation of

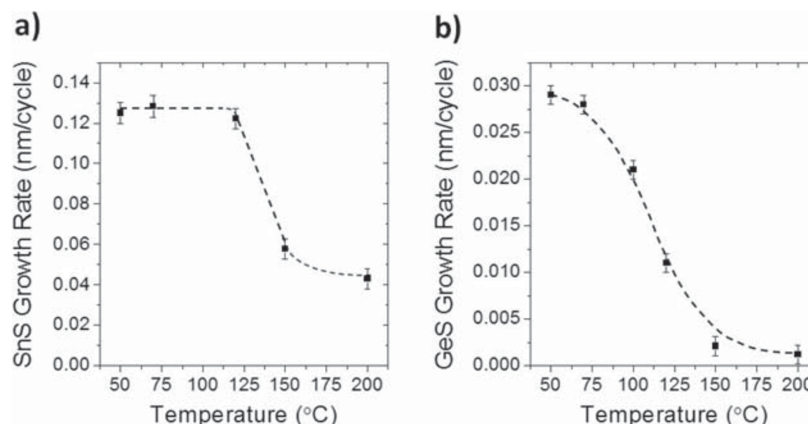

Figure 3. Film growth rate as a function of substrate temperature: (a) SnS (from **2**) and (b) GeS (from **1**).

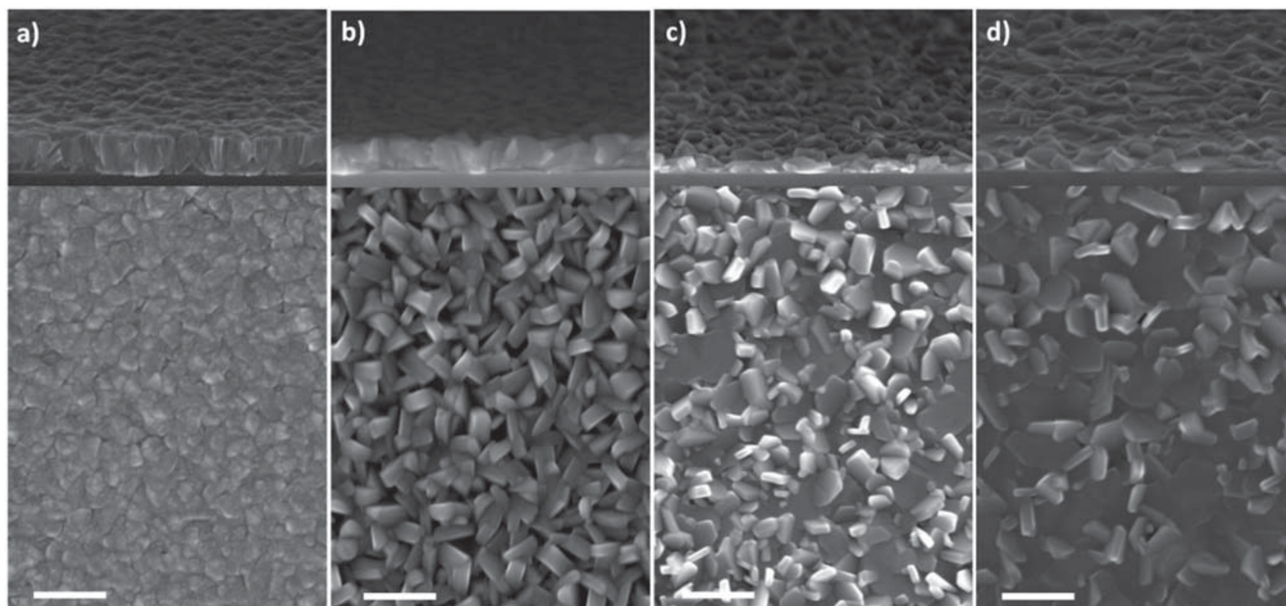

Figure 4. SEM images (top view and side view, scale bar: 250 nm) of SnS films (1000 cycles of **2** and H_2S) at temperatures of (a) 70 °C, (b) 120 °C, (c) 150 °C, and (d) 200 °C.

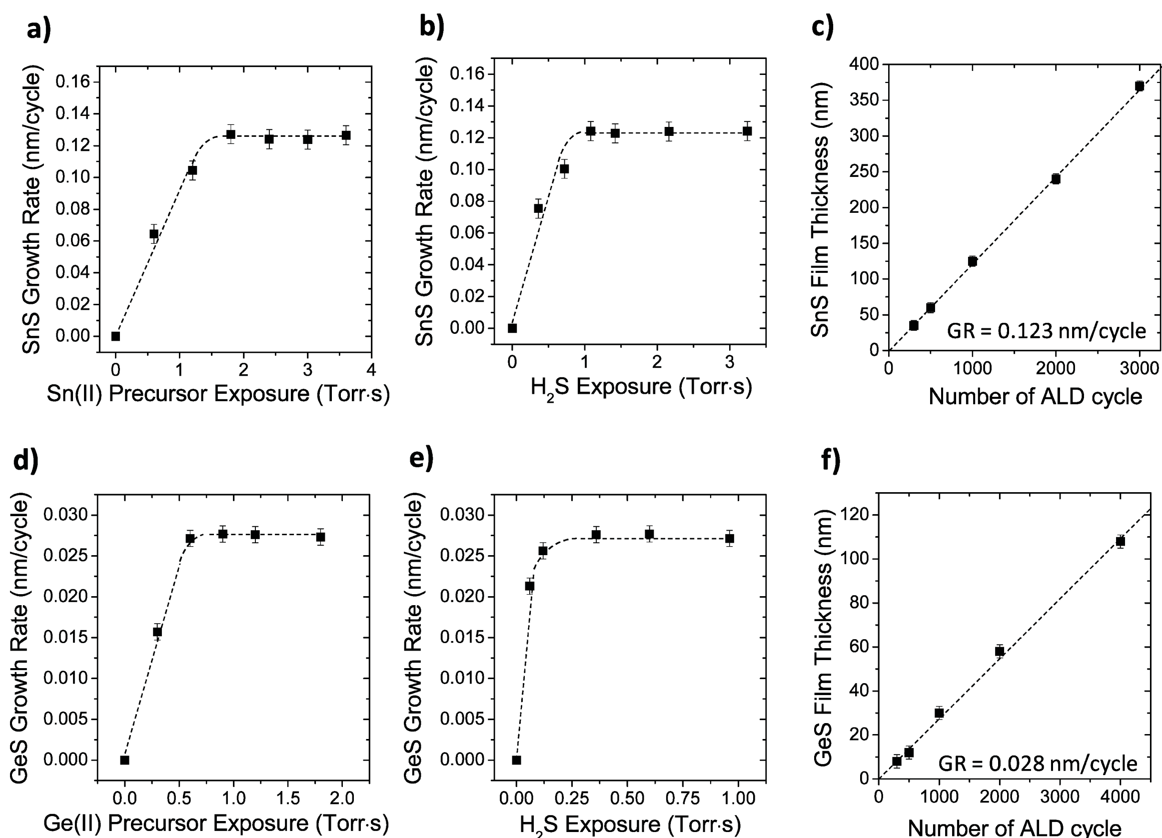

Figure 5. Data showing that film growth rate at constant temperature approaches a constant value (saturated, self-limiting surface reaction) as doses of precursor are increased. (a) Growth rate of SnS films with **2** at fixed H_2S exposure of 2.2 Torr·s. (b) Growth rate of SnS films with H_2S at fixed **2** exposure of 2.4 Torr·s. (c) The thickness of SnS films on SiO_2 substrates using 1.8 Torr·s of **2** and 1.1 Torr·s of H_2S exposure as a function of the number of ALD growth cycles at 70 °C: the linear relationship between metal sulfide film thickness and the number of deposition cycles. (d) Growth rate of GeS films with **1** at fixed H_2S exposure of 0.96 Torr·s, e) Growth rate of GeS films with H_2S at fixed **1** exposure of 0.90 Torr·s. (f) The thickness of GeS films on SiO_2 substrates using 0.60 Torr·s of **1** and 0.96 Torr·s of H_2S as a function of the number of ALD cycles at 70 °C: the linear relationship between metal sulfide film thickness and the number of deposition cycles.

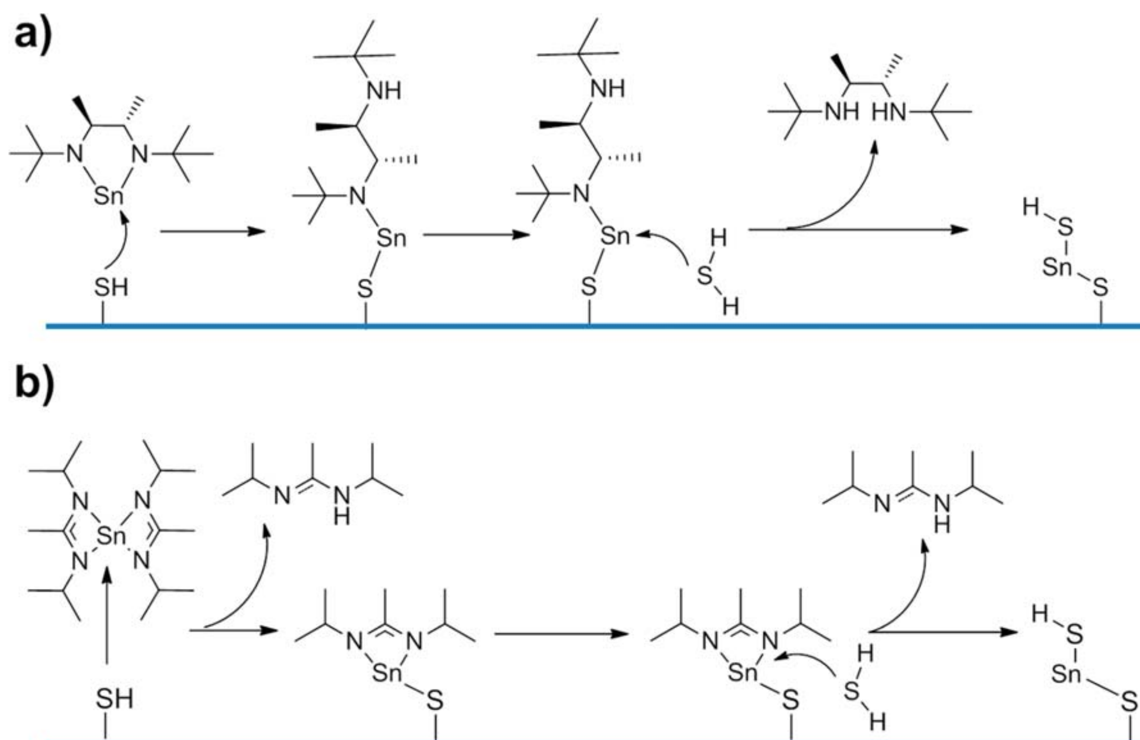

Figure 6. Proposed mechanisms for the formation of SnS films (a) from **2** and (b) **3**.

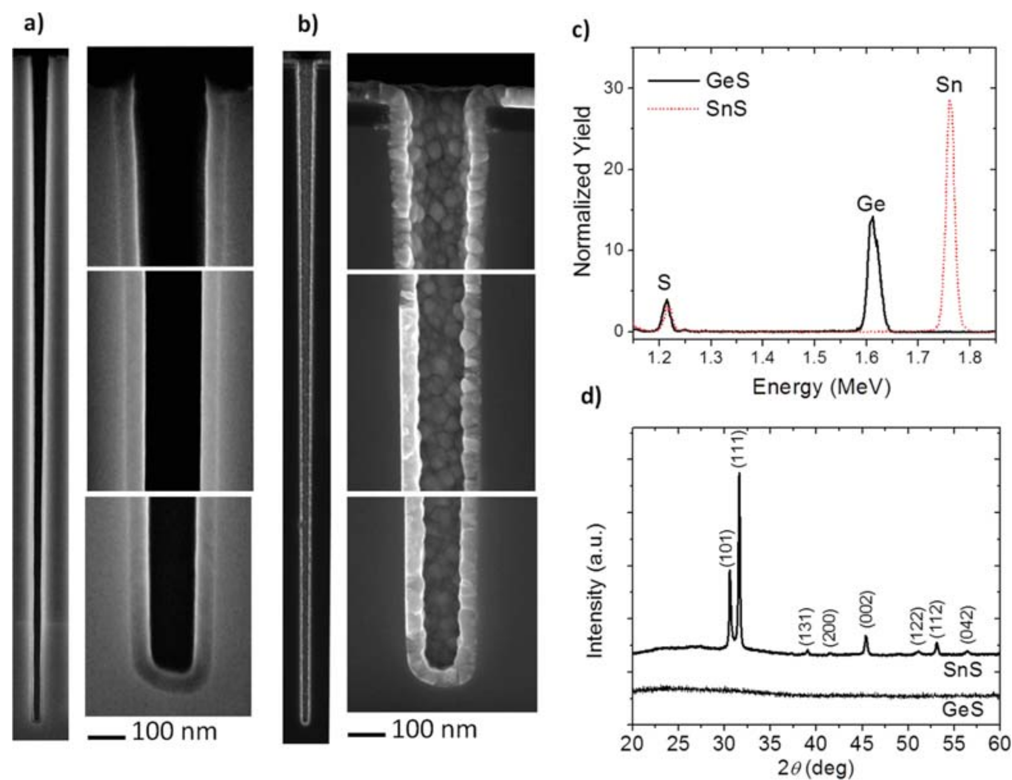

Figure 7. Cross-sectional SEM images of a hole with aspect ratio of ~40:1 coated by (a) GeS, (b) SnS at 70 °C and magnified views of the top, middle, bottom of the coated hole. (c) RBS spectra; (red dotted line) SnS, (black solid line) GeS. (d) XRD spectra of SnS and GeS films.

the growth rate was shown by increasing exposure in Figure 5a, 5b, 5d, 5e. The exposure (product of partial pressure and exposed time) is the total flux of the precursor to the surface that causes the surface reaction to go to completion. Figure 5a show that **2** undergoes self-limiting reactions with the surface prepared by the H_2S. In this experiment (Figure 5a), exposure

dx.doi.org/10.1021/cm403901y | *Chem. Mater.* 2014, 26, 3065−3073

of H_2S was fixed at 2.2 Torr·s. It was found that the saturation of growth rate by **2** starts when its exposure is at *ca.* 1.8 Torr·s. Figure 5b shows that H_2S also undergoes self-limiting reactions with the surface prepared by **2** whose exposure is fixed at 2.2 Torr·s. The saturation of growth rate by H_2S starts when its exposure is at *ca.* 1.1 Torr·s. By comparing the saturation points of each **2** (1.8 Torr·s, Figure 5a) and H_2S (1.1 Torr·s, Figure 5b), it reveals that higher exposure of **2** than that of H_2S is needed to saturate the ALD reactions. From this observation, it seems that the surface reaction between H_2S and the surface prepared by **2** is more facile than that between **2** and the surface prepared by H_2S. At the minimum exposure of **2** (1.8 Torr·s) and H_2S (1.1 Torr·s) to attain the surface saturation, the relation between the thickness and number of cycles was investigated (Figure 5c). From the slope of thickness versus number of cycles, the ALD growth per cycle of SnS from **2** and H_2S was determined to be 1.23 Å/cycle.

Figure 5d shows that the Ge precursor (**1**) undergoes self-limiting reactions with the surface prepared by H_2S with fixed exposure at 0.96 Torr·s. It was found that saturation of the growth rate by **1** starts when its exposure is at *ca.* 0.60 Torr·s. Figure 5e shows that H_2S also undergoes self-limiting reactions with the surface prepared by **1** at a fixed exposure of 0.90 Torr·s. The saturation of growth rate by H_2S starts when its exposure is at *ca.* 0.30 Torr·s. From the comparison of the saturation points of each **1** (0.60 Torr·s, Figure 5d) and H_2S (0.30 Torr·s, Figure 5e), it can be seen that higher exposure of **1** than that of H_2S is needed for surface saturation reaction. From this observation, it seems, as in the case with **2** and H_2S, that the surface reaction between H_2S and the surface prepared by **1** is more facile than that between the Ge precursor (**1**) and the surface prepared by H_2S. The growth rate during ALD of GeS was obtained at 0.60 Torr·s of **1** and 0.96 Torr·s of H_2S exposure and determined to be 0.28 Å/cycle (Figure 5f).

In the case of a tin(II) amidinate complex (**3**), two nitrogen atoms of an amidinate ligand still coordinate to tin after **3** reacts with thiol on the surface (Figure 6). Whereas, after cyclic tin amide (**2**) reacts with thiol on the surface, one nitrogen atom is released from tin and one side of the ligand can rotate freely. Therefore, after surface reaction, the product of **2** can be expected to occupy less surface space versus the surface reaction product of **3**. Thus, it is reasonable that the cyclic complexes **2** (Scheme 1) can react with a higher density of surface sites compared to **3**[51−53] (Scheme 1). This difference may be a reason for the difference in the observed ALD growth rate of SnS film between **2** (1.23 Å/cycle) and **3** (0.90 Å/cycle).[42] However, this steric bulk argument does not explain why GeS grows at a much slower rate (0.28 Å/cycle) from **1** than SnS does from compound **2**, which has a similar structure.

Figure 7a and 7b show cross-sectional SEMs of SnS and GeS deposited at 70 °C inside a deep hole with an aspect ratio of ∼40:1. The images show a uniform, conformal coating indicating self-limiting ALD reactions. It was found by Rutherford backscattering (RBS) that the Sn/S atomic ratio in SnS film was 1:1 and that the Ge/S atomic ratio in GeS film was 1:0.85 (Figure 7c). The XRD spectrum of SnS films shown in Figure 7d exhibits polycrystalline orthorhombic structured SnS (JCPDS# 39-0354).[54,55] No peaks were found in the XRD of GeS, indicating that it is amorphous.

4. CONCLUSIONS

Cyclic Ge(II) amide (**1**) and Sn(II) amide (**2**) complexes were synthesized by the reaction of $M(II)Cl_2$ (M = Ge, Sn) and the *in situ* prepared lithium salt of the ligand. By using an *in situ* synthetic method, synthesis of these complexes could be simplified compared to previously reported methods. GeS films and SnS films were successfully formed using **1** and **2** with H_2S. Those films were formed even inside the holes having a high aspect ratio (∼40:1) with uniformity and conformality. By producing **2** that has a relatively low temperature ALD window range (50−125 °C), ALD of SnS is possible at temperatures from 50 to 250 °C in combination with the Sn(II) amidinate (**3**) (ALD window: 100−250 °C).

■ ASSOCIATED CONTENT

Supporting Information

Photographic image of complexes (**1**, **2**, **3**), ^{1}H, ^{13}C NMR, and X-ray crystallographic files in CIF format for the structure determinations of the two compounds in Table S1. This material is available free of charge via the Internet at http://pubs.acs.org.

■ AUTHOR INFORMATION

Corresponding Author

*E-mail: gordon@chemistry.harvard.edu.

Author Contributions

⊥These authors contributed equally.

Notes

The authors declare no competing financial interest.

■ ACKNOWLEDGMENTS

This work was supported by the U.S. National Science Foundation under NSF Award No. CBET-1032955, the U.S. Department of Energy SunShot Initiative under Contract No. DEEE0005329. ASH acknowledges the Camille and Henry Dreyfus Foundation for support as an Environmental Chemistry Postdoctoral Fellow. This work was performed in part at Harvard University's Center for Nanoscale Systems (CNS), a member of the National Nanotechnology Infrastructure Network (NNIN), which is supported by the National Science Foundation under NSF Award No. ECS-0335765.

■ REFERENCES

(1) Anne, M.-L.; Keirsse, J.; Nazabal, V.; Hyodo, K.; Inoue, S.; Boussard-Pledel, C.; Lhermite, H.; Charrier, J.; Yanakata, K.; Loreal, O.; Le Person, J.; Colas, F.; Compère, C.; Bureau, B. *Sensors* **2009**, *9*, 7398.

(2) Heo, J.; Kim, S. B.; Gordon, R. G. *Appl. Phys. Lett.* **2012**, *101*, 113507.

(3) Heo, J.; Kim, S. B.; Gordon, R. G. *J. Mater. Chem.* **2012**, *22*, 4599.

(4) Heo, J.; Liu, Y.; Sinsermsuksakul, P.; Li, Z.; Sun, L.; Noh, W.; Gordon, R. G. *J. Phys. Chem. C* **2011**, *115*, 10277.

(5) Heo, J.; Hock, A. S.; Gordon, R. G. *Chem. Mater.* **2010**, *22*, 4964.

(6) Gordon, R. *J. Non-Cryst. Solids* **1997**, *218*, 81.

(7) Rosental, A.; Tarre, A.; Gerst, A.; Sundqvist, J.; Hårsta, A.; Aidla, A.; Aarik, J.; Sammelselg, V.; Uustare, T. *Sens. Actuators, B* **2003**, *93*, 552.

(8) Martinson, A. B. F.; Elam, J. W.; Liu, J.; Pellin, M. J.; Marks, T. J.; Hupp, J. T. *Nano Lett.* **2008**, *8*, 2862.

(9) Lee, Y. S.; Heo, J.; Siah, S. C.; Mailoa, J. P.; Brandt, R. E.; Kim, S. B.; Gordon, R. G.; Buonassisi, T. *Energy Environ. Sci.* **2013**, *6*, 2112.

(10) Lee, Y. S.; Heo, J.; Winkler, M. T.; Siah, S. C.; Kim, S. B.; Gordon, R. G.; Buonassisi, T. *J. Mater. Chem. A* **2013**, *1*, 15416.

(11) Antunez, P. D.; Buckley, J. J.; Brutchey, R. L. *Nanoscale* **2011**, *3*, 2399.

(12) Lee, S.-H.; Jung, Y.; Agarwal, R. *Nat. Nano* **2007**, *2*, 626.

(13) Lee, S. Y.; Park, Y. S.; Yoon, S. M.; Jung, S. W.; Yu, B. G. *Electron. Lett.* **2010**, *46*, 652.
(14) Pore, V.; Hatanpää, T.; Ritala, M.; Leskelä, M. *J. Am. Chem. Soc.* **2009**, *131*, 3478.
(15) Pore, V.; Knapas, K.; Hatanpää, T.; Sarnet, T.; Kemell, M.; Ritala, M.; Leskelä, M.; Mizohata, K. *Chem. Mater.* **2010**, *23*, 247.
(16) Knapas, K.; Hatanpää, T.; Ritala, M.; Leskelä, M. *Chem. Mater.* **2009**, *22*, 1386.
(17) Zhang, J.; Wang, X.; Wang, X.; Ma, H.; Cheng, K.; Fan, Z.; Li, Y.; Ji, A.; Yang, F. *Appl. Phys. Lett.* **2010**, *96*, 213505.
(18) Kwon, Y.; Kim, J.-H.; Chae, S.; Lee, Y.; Kim, S. G.; Ku, J.; Sohn, Y.; Park, S. *J. Kor. Phys. Soc.* **2011**, *59*, 466.
(19) Yeung, F.; Ahn, S.-J.; Hwang, Y.-N.; Jeong, C.-W.; Song, Y.-J.; Lee, S.-Y.; Lee, S.-H.; Ryoo, K.-C.; Park, J.-H.; Shin, J.-M.; Jeong, W.-C.; Kim, Y.-T.; Koh, G.-H.; Jeong, G.-T.; Jeong, H.-S.; Kim, K. *Jpn. J. Appl. Phys.* **2005**, *44*, 2691.
(20) Rajendra, B. V.; Kekuda, D. *J. Mater. Sci.: Mater. Electron.* **2012**, *23*, 1805.
(21) Ma, W.; Luther, J. M.; Zheng, H.; Wu, Y.; Alivisatos, A. P. *Nano Lett.* **2009**, *9*, 1699.
(22) Ramasamy, K.; Malik, M. A.; O'Brien, P. *Chem. Commun.* **2012**, *48*, 5703.
(23) Barkhouse, D. A. R.; Gunawan, O.; Gokmen, T.; Todorov, T. K.; Mitzi, D. B. *Prog. Photovoltaics* **2012**, *20*, 6.
(24) Sinsermsuksakul, P.; Hartman, K.; Kim, S. B.; Heo, J.; Sun, L.; Park, H. H.; Chakraborty, R.; Buonassisi, T.; Gordon, R. G. *Appl. Phys. Lett.* **2013**, *102*, 053901.
(25) Sun, L.; Haight, R.; Sinsermsuksakul, P.; Kim, S. B.; Park, H. H.; Gordon, R. G. *Appl. Phys. Lett.* **2013**, *103*, 181904.
(26) Greyson, E. C.; Barton, J. E.; Odom, T. W. *Small* **2006**, *2*, 368.
(27) Jiang, T.; Ozin, G. A. *J. Mater. Chem.* **1998**, *8*, 1099.
(28) Alexandros, S.; Jason, M. S.; Christopher, A. C.; Andrew, G. C.; Patrick, S. G.; Andrew, A. R. W. *Nanotechnology* **2010**, *21*, 185202.
(29) Sinsermsuksakul, P.; Chakraborty, R.; Kim, S. B.; Heald, S. M.; Buonassisi, T.; Gordon, R. G. *Chem. Mater.* **2012**, *24*, 4556.
(30) Kim, J. Y.; George, S. M. *J. Phys. Chem. C* **2010**, *114*, 17597.
(31) Bernardes-Silva, A. C.; Mesquita, A. F.; de Moura Neto, E.; Porto, A. O.; de Lima, G. M.; Ardisson, J. D.; Lameiras, F. S. *Solid State Commun.* **2005**, *135*, 677.
(32) Liu, S.; Guo, X.; Li, M.; Zhang, W.-H.; Liu, X.; Li, C. *Angew. Chem., Int. Ed.* **2011**, *50*, 12050.
(33) Mathews, N. R. *Solar Energy* **2012**, *86*, 1010.
(34) Knez, M.; Nielsch, K.; Niinistö, L. *Adv. Mater.* **2007**, *19*, 3425.
(35) George, S. M. *Chem. Rev.* **2009**, *110*, 111.
(36) Li, W.; Hill, N. J.; Tomasik, A. C.; Bikzhanova, G.; West, R. *Organometallics* **2006**, *25*, 3802.
(37) Tomasik, A. C.; Hill, N. J.; West, R. *J. Organomet. Chem.* **2009**, *694*, 2122.
(38) Mansell, S. M.; Herber, R. H.; Nowik, I.; Ross, D. H.; Russell, C. A.; Wass, D. F. *Inorg. Chem.* **2011**, *50*, 2252.
(39) Li, Z.; Lee, D. K.; Coulter, M.; Rodriguez, L. N. J.; Gordon, R. G. *Dalton Trans.* **2008**, *0*, 2592.
(40) Gordon, R. G.; Hock, A. S.; Heo, J.; Sinsermsuksakul, P. Provisional application No. 61/320,069, filed on Apr. 1, 2010; US patent application No. 13/077,241, filed on Mar. 31, 2011; Pub. No.: US 2012/0027937 A1, Pub. Date: Feb. 2, 2012.
(41) Heo, J.; Hock, A. S.; Gordon, R. G. *Proc. AVS Atomic Layer Deposition Conf.* 2010.
(42) Sinsermsuksakul, P.; Heo, J.; Noh, W.; Hock, A. S.; Gordon, R. G. *Adv. Energy Mater.* **2011**, *1*, 1116.
(43) Cassir, M.; Goubin, F.; Bernay, C.; Vernoux, P.; Lincot, D. *Appl. Surf. Sci.* **2002**, *193*, 120.
(44) Putkonen, M.; Sajavaara, T.; Niinistö, L.; Keinonen, J. *Anal. Bioanal. Chem.* **2005**, *382*, 1791.
(45) Bakke, J. R.; Pickrahn, K. L.; Brennan, T. P.; Bent, S. F. *Nanoscale* **2011**, *3*, 3482.
(46) Kliegman, J. M.; Barnes, R. K. *Tetrahedron* **1970**, *26*, 2555.
(47) Mistryukov, E. A. *Mendeleev Commun.* **2006**, *16*, 258.
(48) Hausmann, D. M.; de Rouffignac, P.; Smith, A.; Gordon, R.; Monsma, D. *Thin Solid Films* **2003**, *443*, 1.
(49) Gordon, R. G. *J. Chem. Phys.* **1962**, *37*, 2587.
(50) Karuturi, S. K.; Liu, L. J.; Su, L. T.; Zhao, Y.; Fan, H. J.; Ge, X. C.; He, S. L.; Yoong, A. T. I. *J. Phys. Chem. C* **2010**, *114*, 14843.
(51) Zydor, A.; Kessler, V. G.; Elliott, S. D. *Phys. Chem. Chem. Phys.* **2012**, *14*, 7954.
(52) Puurunen, R. L. *Chem. Vap. Deposition* **2003**, *9*, 249.
(53) Halls, M. D.; Raghavachari, K. *J. Phys. Chem. A* **2004**, *108*, 2982.
(54) Devika, M.; Reddy, N. K.; Ramesh, K.; Gunasekhar, K. R.; Gopal, E. S. R.; Reddy, K. T. R. *Semicond. Sci. Technol.* **2006**, *21*, 1125.
(55) Devika, M.; Reddy, N. K.; Reddy, D. S.; Reddy, S. V.; Ramesh, K.; Gopal, E. S. R.; Gunasekhar, K. R.; Ganesan, V.; Hahn, Y. B. *J. Phys.: Condens. Matter* **2007**, *19*, 306003.